1.3

HIGH-RESOLUTION MESOSCALE SIMULATIONS ON THE ROLE OF SHALLOW AND DEEP CONVECTION ON DUST EMISSION AND TRANSPORT IN A DESERT AREA

Tetsuya Takemi *

Dept. of Environmental Science and Technology, Tokyo Institute of Technology, Yokohama, Japan

1. INTRODUCTION

Understanding the processes of mineral dust emission, transport, and deposition has been an important research issue not only for predicting disastrous influence of dust storms on human lives, agriculture, transportation system, and other industries but also for evaluating the impact of dust aerosol on the global climate system. A lot of research efforts related to dust emission and transport have been conducted from a global-scale, a synoptic-scale, and a mesoscale point of view, since weather disturbances in these scales are considered as major players in regulating the total amount of tropospheric dust especially in midlatitudes. Although synoptic-scale and mesoscale disturbances seem to play a major role in controlling the total amount of dust concentration and transport in source regions of mid-latitude deserts (e.g., Takemi and Seino 2005), small-scale, boundary-layer mixing is also responsible for dust emission (Cakmur and Miller 2004). Diurnal variability of dust mobilization and concentration is responsible for 20–50 % of the total temporal variability in East Asia (Luo et al. 2004). Koch and Renno (2005) estimated that boundary-layer convective motions contribute to about 35 % of the global dust budget.

One of the remarkable features seen in the desert boundary layer is a large diurnal variability due to intense solar heating. In addition, its top reaches over the 4-km height in a Chinese desert (Takemi 1999; Takemi and Satomura 2000). Such deep boundary layers are anticipated to have a close tie with long-range transport of dust especially in the Chinese deserts, since the boundary-layer top over the deserts where the ground elevation is 1 to 1.5 km becomes very close to the level of westerly jet and thus the boundary-layer air may easily be entrained into the jet stream (Iwasaka et al. 2003). Therefore, the diurnal variation of the boundary layer is critical in evaluating the amount of dust on non-stormy days.

A recent study by Takemi et al. (2005) has presented a modeling framework that explicitly resolves organized motions of convective boundary layer for investigating the dynamical processes relevant to dust transport in a fair-weather setting. The study was motivated by an observational work of Yasui et al. (2005) who demonstrated a clear diurnal variation of the dust concentration in the boundary layer from the data of lidar measurements at a desert site of Shapotou, China (at 37.46°N and 104.95°E, 1250 m above the sea level).

In the present study, we will investigate the dynamical processes and mechanisms of dust emission and transport induced by boundary-layer shallow convection and deep cumulus convection under a fair-weather condition which Yasui et al. (2005) observationally examined in detail. For this purpose, we have performed a series of high-resolution simulations explicitly resolving organized convective motions in a mesoscale domain. The present idealized experiments are not intended to closely mimic a real case over the observation site, but rather are intended to capture the essential features of a fair-weather condition in order to demonstrate the fundamental dynamics of micro-scale processes. We discuss the role of boundary-layer and cumulus convection on dust emission and transport from the surface through the boundary layer up to the free troposphere. We further investigate the sensitivity of convective-scale dust transport to model resolutions in the cloud-resolving range. By demonstrating the resolution sensitivity, we present a simple parameterization of convective dust transport in cloud-resolving simulations.

2. MODEL AND EXPERIMENTAL DESIGN

We use the Advanced Regional Prediction System (ARPS) (Xue et al. 2000), a non-hydrostatic cloud model, which includes a dust emission and transport module (Takemi 2005). The model is configured in an idealized way as in Takemi et al. (2005) in order to focus on the fundamental dynamics of convective dust transport under a fair-weather condition. Simulations are conducted in a mesoscale domain of 80 km (east-west) $\times$ 20 km (north-south) $\times$ 18.4 km (vertical) with the periodic condition at the lateral boundaries. The physics parameterizations, the numerical schemes, and the vertical grid size are exactly the same as in Takemi et al. (2005).

In the dust emission-transport module, the vertical dust flux at the surface depends on the fourth power of friction velocity according to the equation presented in Liu and Westphal (2001), and the dust variables are represented as mixing ratios of 'dry' dust (which is simply termed dust)

**Corresponding author's address*: Dr. Tetsuya Takemi, Department of Environmental Science and Technology, Tokyo Institute of Technology, G5-7, 4259 Nagatsuta, Yokohama, Kanagawa 226-8502; Email: takemi@depe.titech.ac.jp

and 'wet' dust scavenged by rainwater (which is termed rain-wet dust) (Takemi 2005). We assume a single particle size of 1.0-μm radius which is considered to represent a small dust particle that would be transported in the long range.

Cloud-resolving simulations are performed typically with a horizontal grid size of *O*(1 km), and hence the first series of numerical experiments employ a horizontal grid size (denoted as Δx) of 500 m along with stretched vertical grids of 20–810 m intervals. The second series of numerical experiments examine the sensitivity to horizontal grid size ranging from 250 m to 4 km.

The initial base state is set to the horizontal averages over the computational area after a 3-day preliminary run starting with the vertical profile of Yinchuan, China, located in the southern Gobi Desert, at 6 LT (local time) 13 April 2002. This horizontally uniform base state is used for initializing the model with random temperature perturbations added below the 1-km height.

3. CONVECTIVE-SCALE DUST TRANSPORT

In the first series of simulations, we perform a set of sensitivity experiments as well as a control (referred to as CONTROL) simulation in order to examine the effects of vertical wind shear (SHEAR, the mid-level shear is increased), upper-level wind speed (WEAK, the wind speeds are uniformly reduced), and moist convection (NOMPHYS, the cloud microphysics parameterization is off).

At first the result from the control simulation is described. In Takemi et al. (2005), it was shown that the simulation reproduced the diurnal variation of fair-weather convective boundary layer commonly seen in a Chinese desert despite the simplified model settings. During the course of this diurnal variation, boundary-layer convection and cumulus cells develop. The convective activity is measured here with the horizontally averaged value and the standard deviation of vertical velocity, which is depicted in Fig. 1. The cloud boundary is defined as a contour of cloud-water plus cloud-ice mixing ratio being 0.01 g kg^{-1}. At around 11 LT, strong updraft develops in the boundary layer, penetrating above the 4-km height to generate convective cloud. This convective cloud activity is also indicated by a large standard deviation of vertical velocity. The rapid development of deep convection at 11 LT is due to the initial stratification having a shallow surface stable layer capped by a thick neutral layer up to the 4-km height: once the shallow stable layer is broken by surface heating, updrafts penetrate through the neutral layer deeply into the free troposphere. After the noon time, owing to the continuous strong surface heating, intense updrafts sporadically develop not only in the boundary layer but also in the cloud layer, as seen from the large means and standard deviations. The cloud layer gradually extends upward until 17 LT, accompanying a moderate amount of the standard deviation.

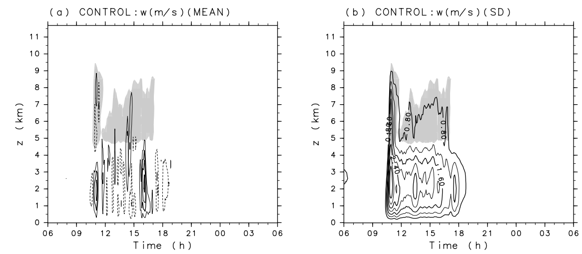

Figure 1: Time-height section of (a) vertical velocity averaged at each horizontal level (contoured at 0.015 m s^{-1}) and (b) its standard deviation (contoured at 0.4 m s^{-1} above 0.8 m s^{-1}) for the CONTROL experiment. The cloud region (defined by the area in which horizontally averaged cloud-water plus cloud-ice mixing ratio exceeds 0.01 g kg^{-1}) is also indicated by gray shading.

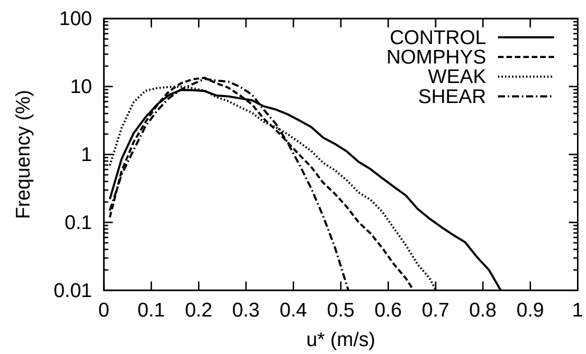

Figure 2: Distribution of friction velocity frequency (in %) during 10–18 LT for all the experiments.

The temporal evolution of the mean vertical distribution of dust as well as vertical dust flux was examined (not shown). At around 11 LT dust was quickly transported upward within the boundary layer, and the dust concentration increased rapidly by the noon time, which were due to the development of intense convection. In the afternoon period, the dust concentration below the cloud-base level (i.e., the 4-km height) continuously increased, and some fraction of the dust was gradually raised above the 4-km height.

Through the sensitivity simulations, the dust transport critically depends on upper-level wind speed, vertical wind shear, and cloud development. This sensitivity is demonstrated in terms of friction velocity in Fig. 2 which compares the frequency distribution of friction velocity during 10–18 LT. It is clearly seen that the frequency distribution is shifted to a weaker velocity range from the control (CONTROL) to the sensitivity experiments (WEAK, NOMPHYS, and SHEAR). This behavior led to the difference in the column total dust.

In order to demonstrate the processes relevant to dust transport, the vertical eddy fluxes of horizontal momentum is examined. Figure 3 shows the time and height sections of the vertical momentum flux as well as the x-

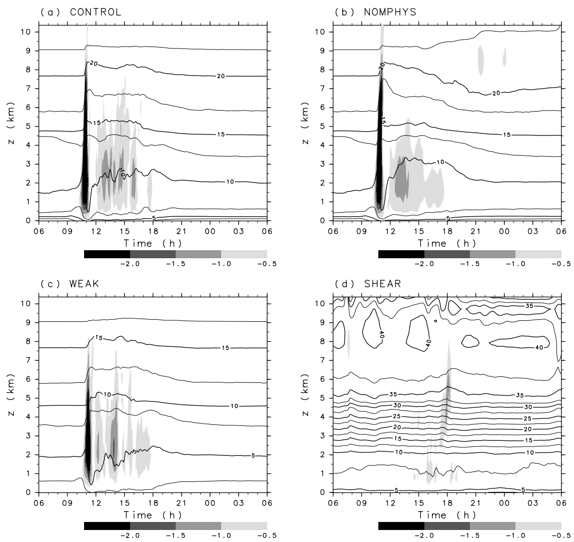

Figure 3: Time-height section of vertical flux of horizontal momentum (in m^2 s^{-2}, shaded, the legend shown in the bottom of each panel) and x-component horizontal wind (contoured at 2.5-m s^{-1} interval) for (a) the CONTROL, (b) the NOMPHYS, (c) the WEAK, and (d) the SHEAR experiments. Only downward fluxes are depicted.

component wind averaged horizontally over the computational area for the first series of numerical experiments. A considerable amount of downward momentum flux is seen at around 11 LT in all the cases except the SHEAR experiment; this is obviously caused by deep penetrating convection that induces abrupt increase in dust concentration. A significant amount of the downward flux continues throughout the afternoon in the three cases. When the result of the NOMPHYS is compared with that of the CONTROL, the activity of the downward flux seems to be significantly weakened in the afternoon and hence is the boundary-layer wind speed. This suggests that cumulus cloud activity has a role of enhancing downward momentum flux. By reducing the base-state horizontal wind speed (i.e., the WEAK case), the wind speed at the surface and in the boundary layer is therefore reduced even with a comparable amount of downward momentum flux with the CONTROL result. By increasing the strength of the shear in the 2–5 km layer (i.e., the SHEAR case), the development of mixed boundary layer is considerably suppressed and shallow, stratiform-type clouds prevail throughout the day. Owing to the absence of convective activity in this case, the vertical momentum flux is considerably reduced.

We have performed a set of sensitivity simulations in order to investigate the fundamental processes of dust emission and transport induced by small-scale processes, i.e., dry and moist convection. The simulations indicated that a weak shear environment in the lower troposphere is favorable for the development of a deep convective boundary layer, which supports the view presented observationally by Yasui et al. (2005). However, a weak wind speed in the low levels (i.e., below the 4-km level) itself does not produce a large amount of dust emission. Our sensitivity experiments clearly demonstrated that a certain amount of wind speed, i.e., the threshold wind speed for dust emission, is at least necessary for the enhancement of surface winds which is due to the downward transport of higher momentum by deep convective motion.

4. RESOLUTION DEPENDENCE AND PARAMETERIZATION

In the second series of simulations, we examine various Δx of 250 m, 500 m, 1 km, 2 km, and 4 km. The case with the smallest grid size, which is sufficient to resolve boundary-layer and cumulus convection, is regarded as the control in this simulation series.

Figure 4 shows the time-height section of horizontally averaged dust concentration, vertical dust flux, and cloud mixing ratio (a proxy for cloud boundary) for the cases with different horizontal resolutions. In the control case (i.e., with $\Delta x = 250$ m), upward dust flux develops at around 10:30 LT and dust is quickly mixed within the boundary layer i.e., below the 4.5-km level. Above the boundary layer develop cumulus clouds, which transport dust further upward into the free troposphere. The significant upward flux continues throughout the afternoon and the dust content gradually increases not only in the boundary layer but in the free troposphere as well. A similar feature is basically found for the cases with the coarser grids except the 4 km-grid case that demonstrates a later but more sudden development of upward dust flux. In addition, the coarsest grid case resulted in the highest value of column integrated dust content. This is due to an unexpectedly sudden and intense cumulus convection that developed during 14–15 LT.

The results indicate that the grid size of 4 km, which is well in the range of explicit representation of moist convection in mesoscale convective systems (Weisman et al. 1997), is not sufficient to resolve shallow and deep convection under a fair-weather condition. Since the 4-km mesh is not so coarse for mesoscale (let alone global-scale) simulations of convective dust transport and moreover most studies aim at performing simulations with grid size of 1–10 km, a proper parameterization for activating convection that leads to dust emission and transport is necessary in this range of grid size. For this purpose, we apply the idea of Deng et al. (2003) who developed a shallow-convection parameterization in mesoscale models. They hypothesized that cloud-forming rising parcels were positively correlated with vertical velocity perturbations and defined eddy vertical velocity in terms of turbulent kinetic energy (TKE) to be added to resolved vertical motion.

On the basis of their hypothesis, we assume that updraft is enhanced through eddy motion in an appropriate

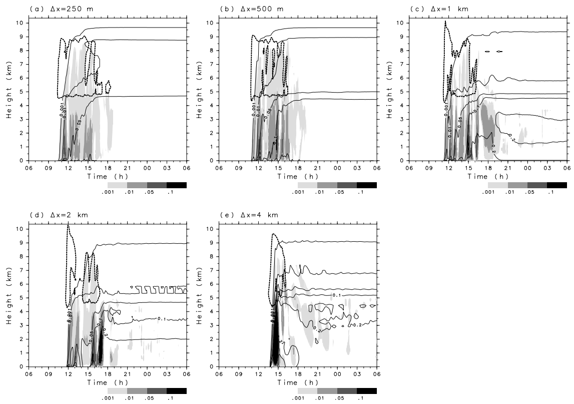

Figure 4: Time-height section of area-averaged dust concentration (contoured at 0.001, 0.01, 0.05, 0.1, and 0.2 mg m^{-3}), upward flux of dust (shaded, in mg m^{-2} s^{-1}), and cloud boundary (dotted, the contour of 0.01 g kg^{-1} of cloud water plus ice mixing ratio) with Δx of (a) 250 m, (b) 500 m, (c) 1 km, (d) 2 km, and (e) 4km.

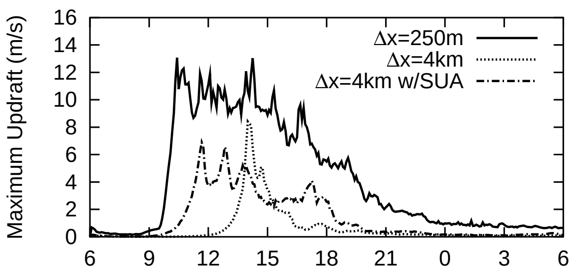

Figure 5: Temporal variation of the maximum updraft in the domain for the cases of 250 m-grid, 4 km-grid, and 4 km-grid with SUA.

time scale: in the updraft regions a forcing term is added to the vertical momentum equation. This term is referred to as subgrid-scale updraft acceleration (SUA) and is written as:

$$\left(\frac{dw}{dt}\right)_{\mathrm{SUA}} = \frac{1}{\tau}\sqrt{\frac{2}{3}e}, \tag{1}$$

where w is vertical velocity, e is TKE, and τ is the timescale for the updraft acceleration. By trial and error we set $\tau = 10$ min.

The temporal variation of the maximum upward velocity in the domain is compared in Figure 5. Although the velocity in the 4 km-grid case with SUA is weaker than that in the 250 m-grid case, adding the forcing term overall improves the velocity variation. By examining the distribution of the frequency of surface wind speed, we found that the distribution in the case of 4-km grid with SUA better captured the feature in the 250 m-grid case than without the parameterization.

With the boundary-layer development and associated surface wind variation being better represented with the SUA parameterization, the convective dust emission and transport is significantly improved. Figure 6 demonstrates

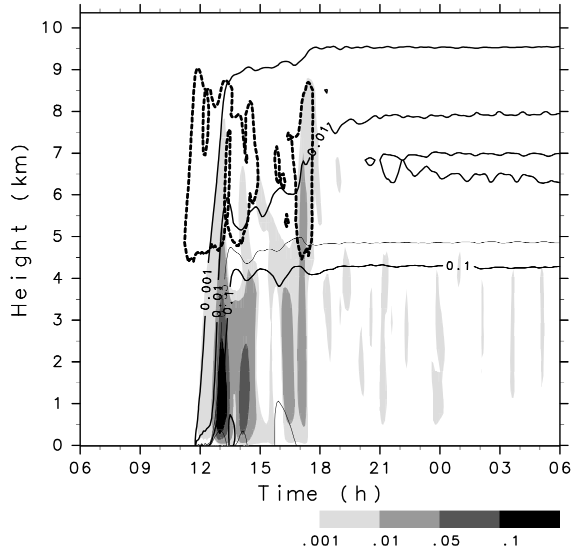

Figure 6: The same as Figure 4, except for the case of $\Delta x = 4$ km with subgrid-scale updraft acceleration.

that the diurnal development of vertical dust transport with SUA compares well with the fine-mesh case shown in Figure 4a. Therefore, a simple representation using TKE for accelerating vertical velocity depicted in (1) can be used for cloud-resolving simulations of convective dust transport.

5. CONCLUSIONS

Shallow convection plays a primary role in vertically mixing dust within the boundary layer. If deep cumulus convection also comes into play, mass concentration of dust increases not only within the boundary layer but also in the free troposphere. A coupled effect of dry and moist convection is important because convection is more enhanced with the coupled effect than without moist processes. Furthermore, transports upper-level higher momentum down to the surface, intensifying surface winds and hence dust emission. A wind speed exceeding the threshold for surface dust emission is necessary at the upper levels of the daytime boundary layer for the surface wind enhancement. Although the amount of dust lifted is much smaller during a single diurnal cycle of fair weather than associated with a single case of synoptic disturbances, the total amount of dust emission due to fair-weather processes may not be neglected in a longer time-scale.

A significant difference between the coarse- and fine-resolution simulations is found in the column amount of dust floating in the air. The results of the higher-resolution simulations have been further compared with those of low-resolution simulations with a grid size of *O*(1 km). The subgrid-scale mixing due to a turbulence parameterization seems to be effective in the cases with the grid size of 500 m and lower. In order to properly represent the convective dust transport under a fair-weather condition in cloud-resolving simulations, the development of shallow and deep convection should be well resolved. Our sensitivity simulations to horizontal grid size suggested that a parameterization that activate shallow and deep convection needs to be included in simulations with a grid size of 1-10 km. We present a simple formulation of convective dust transport in cloud-resolving simulations with that range of grid size.

6. ACKNOWLEDGMENT

This study was supported by Japan Society for the Promotion of Science under Grant-in-Aid for Scientific Research 17740304. The ARPS model was developed by the Center for Analysis and Prediction of Storms (CAPS), The University of Oklahoma. CAPS is supported by the National Science Foundation and the Federal Aviation Administration through combined grant ATM92-20009.

7. REFERENCES

Cakmur, R. V., and R. L. Miller, 2004: Incorporating the effect of small-scale circulations upon dust emission in an atmospheric general circulation model. *J. Geophys. Res.*, **109**, D07201, doi:10.1029/2003JD004067.

Deng, A., N. L. Seaman, and J. S. Kain, 2003: A shallow-convection parameterization for mesoscale models. Part I: Submodel description and preliminary applications. *J. Atmos. Sci.*, **60**, 34–56.

Iwasaka, Y., T. Shibata, T. Nagatani, G. Y. Shi, Y. S. Kim, A. Matsuki, D. Trochkine, D. Zhang, M. Yamada, M. Nagatani, H. Nakata, Z. Shen, G. Li, B. Chen, and K. Kawahira, 2003: Large depolarization ratio of free tropospheric aerosols over the Taklamakan Desert revealed by lidar measurements: Possible diffusion and transport of dust particles. *J. Geophys. Res.*, **108**, 8652, doi:10.1029/2002JD003267.

Koch, J., and N. O. Renno, 2005: The role of convective plumes and vortices on the global aerosol budget. *Geophys. Res. Lett.*, **32**, L18806, doi:10.1029/2005GL023420.

Liu, M., and D. L. Westphal, 2001: A study of the sensitivity of simulated mineral dust production to model resolution. *J. Geophys. Res.*, **106**, 18099–18112.

Luo, C., N. Mahowald, and C. Jones, 2004: Temporal variability of dust mobilization and concentration in source regions. *J. Geophys. Res.*, **109**, D20202, doi:10.1029/2004JD004861.

Takemi, T., 2005: Explicit simulations of convective-scale transport of mineral dust in severe convective weather. *J. Meteor. Soc. Japan*, **83A**, 187–203.

Takemi, T., 1999: Structure and evolution of a severe squall line over the arid region in northwest China. *Mon. Wea. Rev.*, **127**, 1301–1309.

Takemi, T., M. Yasui, J. Zhou, and L. Liu, 2005: Modeling study of diurnally varying convective boundary layer and dust transport over desert regions. *SOLA*, **1**, 157–160.

Takemi, T., and N. Seino, 2005: Dust storms and cyclone tracks over the arid regions in east Asia in spring. *J. Geophys. Res.*, **110**, D18S11, doi:10.1029/2004JD004698.

Takemi, T., and T. Satomura, 2000: Numerical experiments on the mechanisms for the development and maintenance of long-lived squall lines in dry environments. *J. Atmos. Sci.*, **57**, 1718–1740.

Weisman, M. L., W. C. Skamarock, and J. B. Klemp, 1997: The resolution dependence of explicitly modeled convective systems. *Mon. Wea. Rev.*, **125**, 527–548.

Xue, M., K. K. Droegemeier, and V. Wong, 2000: The Advanced Regional Prediction System (ARPS) - A multiscale nonhydrostatic atmospheric simulation and prediction tool. Part I: Model dynamics and verification. *Meteor. Atmos. Physics*, **75**, 161–193.

Yasui, M., J. Zhou, L. Liu, T. Itabe, K. Mizutani, and T. Aoki, 2005: Vertical profiles of aeolian dust in the desert atmosphere observed by a lidar in Shapotou, China. *J. Meteor. Soc. Japan*, **83A**, 149–171.